Optimization methods for 3D lithography process utilizing DMD-based maskless grayscale photolithography system

Ma, X; Kato, Y; Hirai, Y; van Kempen, Floris; van Keulen, Fred; Tsuchiya, T; Tabata, O

DOI
10.1117/12.2084486

Publication date
2015

Document Version
Final published version

Published in
Optical Microlithography XXVIII

Optimization methods for 3D lithography process utilizing DMD-based maskless grayscale photolithography system

Xiaoxu Ma*[a], Yoshiki Kato[a], Yoshikazu Hirai[a], Floris van Kempen[b], Fred van Keulen[b], Toshiyuki Tsuchiya[a], Osamu Tabata[a]
[a]Dept. of Micro Engineering, Kyoto University, Kyoto daigaku-Katsura, Nishikyo-ku, Kyoto 615-8540, Japan; [b]Dept. of Precision and Microsystems Engineering, Delft University of Technology, Mekelweg 2, 2628 CD Delft, The Netherlands

ABSTRACT

Digital Micromirror Device (DMD)-based grayscale lithography is a promising tool for three dimensional (3D) microstructuring of thick-film photoresist since it is a maskless process, provides possibility for the free-form of 3D microstructures, and therefore rapid and cost-effective microfabrication. However, process parameter determination lacks efficient optimization tool, and thus conventional look-up table (indicating the relationship between development depth and exposure dose value under a fixed development time) approach with manual try-and-error adjustment is still gold standard. In this paper, we firstly present a complete "input target-output parameters" single exposure optimization method for 3D microstructuring utilizing DMD-based grayscale lithography. This numerical optimization based on lithography simulation and sensitivity analysis can automatically optimize a combination of three process parameters for target microstructure; exposure dose pattern, a focal position, and development time. Through a series of experiments using a 20 μm thick positive photoresist, validity of the proposed optimization approach has been successfully verified. Secondly, with the purpose of further advancing accuracy and improve the uniformity of precision for the target area, a multiple exposure optimization method is proposed. The simulated results proved that the multiple exposure optimization method is a promising strategy to further improve precision for thicker photoresist structure.

Keywords: 3D microstructuring, 3D photolithography, DMD-based grayscale lithography, Optimization, Lithography simulation, Thick photoresist, Fast Marching Method

1. INTRODUCTION

Three-dimensional (3D) photolithography provides a patterning solution for free-form 3D microstructures in thick-film photoresist in contrast to binary lithography, which is widely accepted for the integrated circuit (IC) industry only produces planar structures. 3D photolithography has become important technology for many Micro Electro Mechanical Systems (MEMS) application fields [1][2]. Usually, 3D photoresist microstructure is realized by using a gray tone UV exposure technique to control the development rate, and therefore the final development depth in photoresist. Several approaches for grayscale lithography has been proposed such as grayscale mask lithography [3], moving-mask UV lithography [4], and digital micromirror device (DMD)-based grayscale lithography [5]-[7]. Among many grayscale lithography approaches, DMD-based grayscale lithography has recently been receiving much attention because DMD can project the grayscale mask pattern according to the pixel information of a bitmap instead of relying on a high-resolution optical photomask (i.e., maskless approach as shown in Fig. 1a).

On DMD lithography system (Fig. 1b), when matrix-positioned digital micromirror arrays receives signal from computer (i.e., bitmap data, designed exposure dose pattern), they modulates spatial UV light which will finally expose photoresist through a projection optical system. Generally, among the many process parameters in DMD-based grayscale lithography of thick-film positive photoresist, three important process parameters should be determined prior to fabrication: (1) exposure dose pattern associated with grayscale mask pattern, (2) focal position in photoresist, and (3) development time. However, determining these highly coupled process parameters is not an easy task. Several previously reported simulation and optimization techniques for the optical lithography or 3D photolithography are helpful; the conventional approach based on calibrating the relationship between the exposure dose and the resulting photoresist height (i.e., development depth) [8]; the commercially available simulation software in IC industry [9][10]; the authors' previously reported optimization method specific to the parallel optical system [11]. Unfortunately, none of them can

Optical Microlithography XXVIII, edited by Kafai Lai, Andreas Erdmann, Proc. of SPIE Vol. 9426, 94260F
 · doi: 10.1117/12.2084486

satisfy all the following requirements for optimization on DMD-based grayscale lithography: (1) optical lithography model for DMD exposure system, (2) comprehensive understanding on the complete 3D photolithography process of thick photoresist, and (3) realization of an automated optimization process. Thus, the fabricated results of any of the mentioned methods are unacceptable and they should be revised through trial-and-error which is inefficient and time-consuming.

In this paper, a novel optimization method based on single exposure (here after: single exposure optimization method) is first introduced which can automatically determine an accurate combination of the exposure dose pattern, focal position, and development time for the targeted 3D microstructure in thick positive photoresist. After describing the simulation model of DMD-based grayscale lithography, the validity and effectiveness of the proposed optimization method are demonstrated by comparing the simulation and fabrication results. Meanwhile, further improvement of fabrication accuracy is achieved for single critical feature by introducing a variable weight factor, and its usefulness is demonstrated. However, our further analysis indicates that error distribution after optimization is not uniform for the whole target area, and higher accordance can always be achieved around focal position comparing to area out of the depth of focus (DOF) of the optics. Thus, for applications where relatively higher uniformity of fabrication accuracy is required, another optimization method based on multiple exposures (here after: multiple exposure optimization method) is introduced. This multiple exposure optimization method provides a promising strategy to further improve precision for thicker photoresist microstructure.

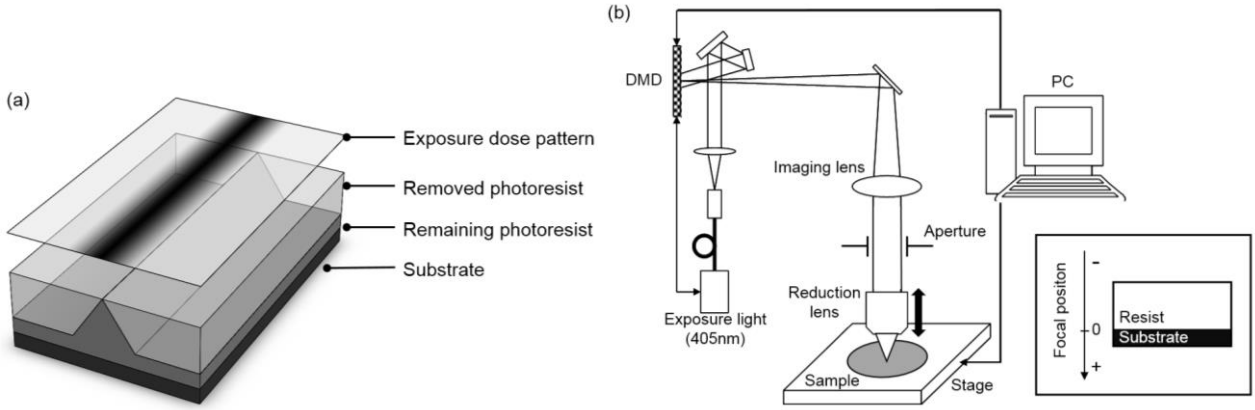

Figure 1. Schematic representation of (a) grayscale lithography, and (b) system structure of DMD-based grayscale lithography apparatus.

2. OPTIMIZATION METHODS

2.1 Single exposure optimization method

The flowchart shown in Fig. 2 summarizes the optimization procedure schematically. The single exposure optimization method consists of exposure simulation, development simulation and a pattern optimizer based on sensitivity analysis with the steepest descent method [12]. Initially, a target 3D microstructure is input into the program. The optimization will be launched by an initially estimated exposure dose pattern for the target microstructure. The optimization performs the following steps:

1. Under a fixed focal position for the entire target area (Fig. 3), calculate the exposure dose distribution $E(\boldsymbol{x})$ inside the photoresist by exposure simulation specific for DMD-based grayscale lithography [13]-[15].
2. Determine local dissolution rate $v(\boldsymbol{x})$ from local exposure dose based on empirical dissolution rate model.
3. Calculate the advancement of the development front (i.e. local development front arrival time $T(\boldsymbol{x})$) using Fast Marching Method (FMM) [16]. Then find the best development time t_{dev} for the target 3D microstructure when fabricated using current exposure dose pattern. The development front under best development time is called as simulated structure.
4. Evaluate error between the simulated microstructure and the target:

$$\varepsilon = \int_{\Gamma_t} w(\mathbf{x})\{v(\mathbf{x})(T(\mathbf{x}) - t_{dev})\}^2 d\Gamma, \quad \mathbf{x} \in \Gamma_t \tag{1}$$

where $w(\mathbf{x})$ is the weight factor and Γ_t is the target microstructure surface. Compare to the accuracy requirement and check whether a stop condition is met, e.g. maximum program running time, minimum step-size of exposure dose pattern.

5. If not, adjust exposure dose pattern using the pattern optimizer and repeat step 1 to 4 until the optimization satisfies the required accuracy or reaches a stop condition. For the latter case, the optimization on exposure dose pattern and development time has come to its limitation.
6. Repeat the above procedure step 1 to 5 for different focal positions to find the minimum error. Finally, the optimization outputs the best combination of exposure dose pattern, focal position and development time.

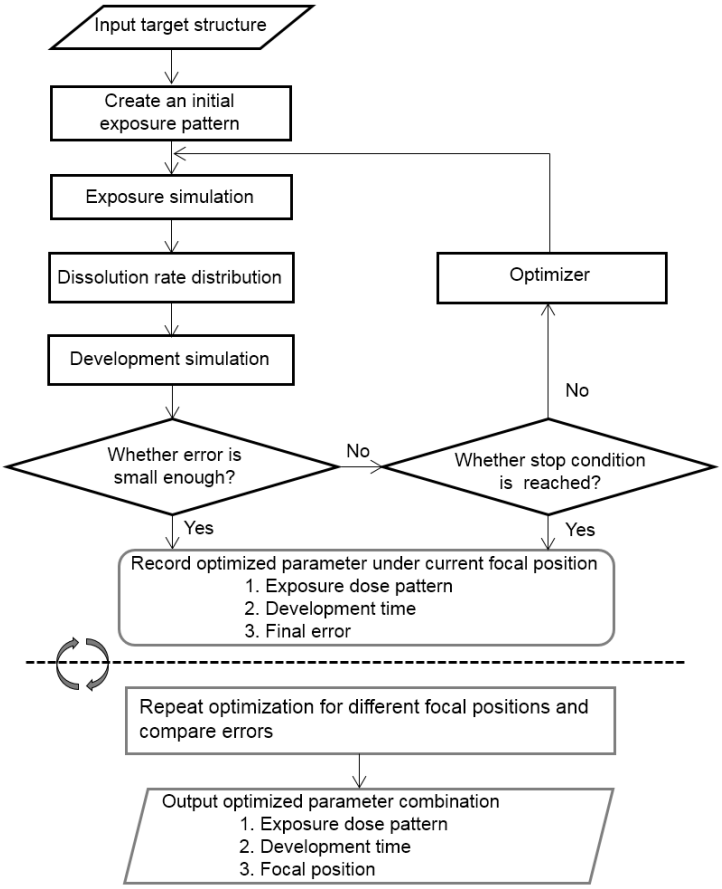

Figure 2. Flowchart showing the basic steps in the single exposure optimization method.

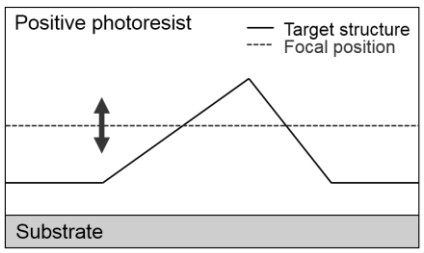

Figure 3. Focal position setting for the single exposure method.

2.2 Multiple exposure optimization method

Multiple exposure optimization method shares the common optimization approach with single exposure optimization method, but adopts a different focal position setting (Fig. 4a): the target microstructure profile is horizontally sliced by its height at a user defined segment interval (less than the DOF). With multiple focal positions assigned at the middle of each sliced area, the exposure dose pattern for the entire target area is optimized. However, for DMD-based grayscale lithography system, only one focal position is allowed for one exposure process. Thus, each sliced area needs to be exposed independently with exposure dose pattern determined by dividing the previously optimized pattern. Figure 4b shows the relationship between the entire exposure dose pattern and divided ones.

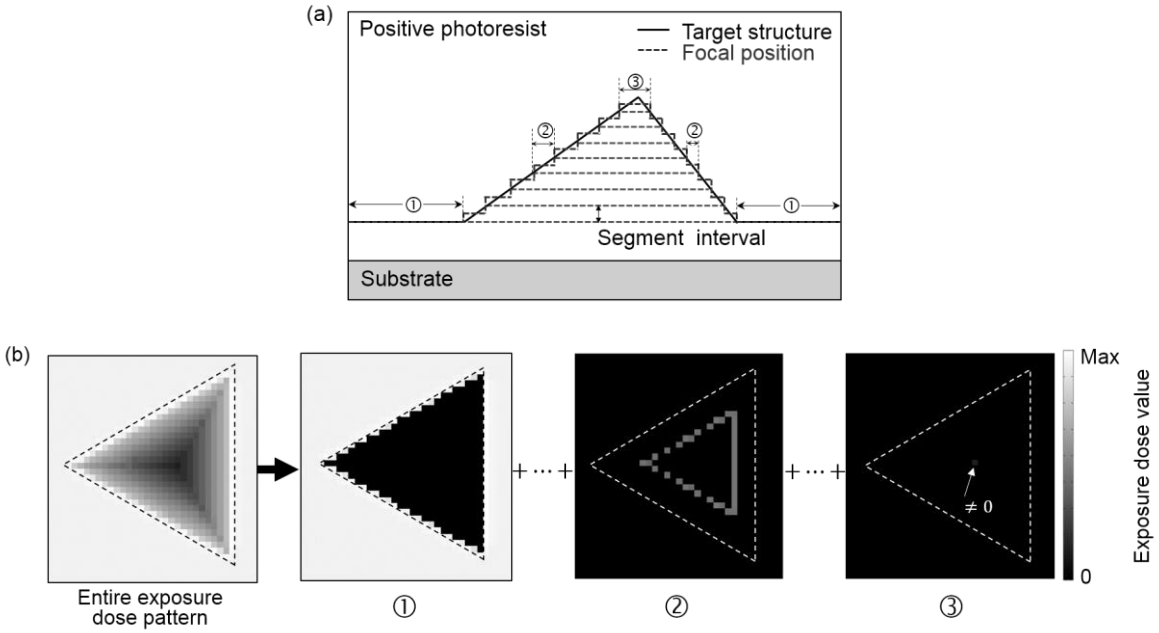

Figure 4. (a) Focal position setting for the multiple exposure optimization method. (b) Entire exposure dose pattern and divided exposure dose patterns. The dashed line stands for the pyramid structure area.

This multiple exposure optimization method is based on a qualitative analysis, revealing that better optimization result can always be achieved around focal position comparing to area out of the DOF. The reason for this phenomena is owing to the actual radiant intensity distribution of emitted light which also functions in the sensitivity analysis in the pattern optimizer. Therefore, exposure dose pattern P can be updated towards the optimizing direction by Eq. 2 with adjoint sensitivity [17] given by Eq. 3:

$$P(k+1) = P(k) - \frac{\partial \varepsilon}{\partial P} \cdot \Delta, \quad k = 0, 1, 2, 3\ldots \tag{2}$$

$$\frac{\partial \varepsilon}{\partial P_i} = \int_{\Gamma_t} 2w(\mathbf{x})v(\mathbf{x})(T(\mathbf{x}) - t_{dev})^2 \frac{\partial v(E(\mathbf{x}))}{\partial E(\mathbf{x})} \frac{I_i(\mathbf{x})}{I_0} d\Gamma + \int_{\Omega_t} \frac{2\mu(\mathbf{x})}{v(\mathbf{x})^3} \frac{\partial v(E(\mathbf{x}))}{\partial E(\mathbf{x})} \frac{I_i(\mathbf{x})}{I_0} d\Gamma \tag{3}$$

where k is the iteration number, Δ is the step-size of exposure dose change, P_i stands for the pattern pixel i, I_i is the radiant intensity corresponding to pattern pixel P_i, Ω_t is the developed area in simulation and μ is the adjoint variable [17]. Figure 5a indicates the domain and boundaries for the integral in Eq. (3). In the pattern optimizer, the target area of which that the precision can be improved by sensitivity is restricted to the target area where local radiant intensity I_i has non-zero value. When the target is far from the *projected* pattern pixels (i.e. pattern pixels added with focal position information), e.g. P_A and P_B (Fig. 5b), each affected target area (a, b) is relatively large and will possibly get superposed (a+b area) when P_A and P_B locate closely. Sensitivities of the two pattern pixels try to reduce the error of the superposed area independently. The independent pattern update for P_A and P_B without consideration for each other's change makes

the final result less predictable (whether error becomes small or not), thus degrades the optimization quality for the superposed area. Meanwhile, when the target is near the projected pattern pixels, e.g. P_C and P_D, the affected area is restrained to a narrower range (c, d) within the DOF receiving less interference from neighboring pattern pixels. Thus, error at (c, d) will be reduced solidly by sensitivities of P_C and P_D. In conclusion, better optimization result can always be achieved around focal position comparing to area out of the DOF, and the multiple exposure optimization method based on this qualitative analysis is reasonable.

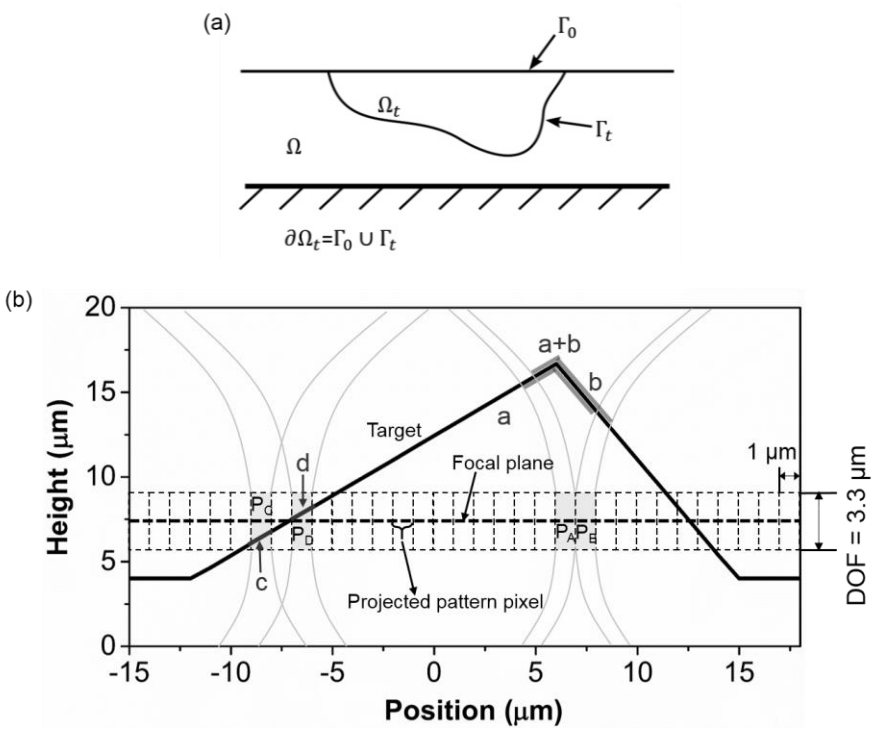

Figure 5. (a) Domain and boundaries for sensitivity analysis. (b) Affected areas of pattern pixels with different position relationships towards the target.

3. EXPERIMENT

Experiment for sample preparation and evaluation were conducted as follows: (1) a 20 μm thick layer of positive photoresist (PMER P-LA900PM, Tokyo Ohka Kogyo Co. Ltd.) was spin-coated on Si wafer, (2) a pre-bake process was performed at 115 °C for 6 min on a hotplate, (3) a relaxation time for photoresist rehydration was provided, (4) an exposure procedure was applied on a DMD exposure system (DL-1000GS/KCH NanoSystems Solutions, Inc.) (Fig. 1b). (5) A development process is carried out by a developer (P-7G, Tokyo Ohka Kogyo Co., Ltd.) for the photoresist using the dip method. (6) Fabricated 3D microstructure is observed by a scanning electron microscope (SEM) and height information of fabricated microstructure is captured by a 3D laser scanning microscope (VX-X200, Keyence Co.). To evaluate fabrication performance, two kinds of error are used: One is the local height difference between measurements and the target ones. The other one is quadratic mean error evaluating result from an over-all perspective.

4. RESULTS AND DISCUSSION

4.1 Measurement of dissolution rate

To demonstrate the accuracy of computational model and verify the proposed optimization method, dissolution rate was first determined by a dedicated method for thick photoresist [18][19]. Local dissolution rate $v(\mathbf{x})$ as a function of local exposure dose value $E(\mathbf{x})$ and depth z, and the experiment data was fitted to the following model proposed by authors group [19], using non-linear regression:

$$v(\mathbf{x}) = g(E(\mathbf{x})) = \begin{cases} 0 \le E(\mathbf{x}) \le 270[\text{mJ/cm}^2] \\ \qquad A'(E(\mathbf{x})) \cdot \exp\{-21.543E(\mathbf{x})^{-0.804} \cdot z\} \\ 270 \le E(\mathbf{x})[\text{mJ/cm}^2] \\ \qquad 4.949 \qquad\qquad\qquad\qquad\qquad\qquad\qquad\qquad\qquad , 0 \le z \le z_{th}(E(\mathbf{x})) \\ \qquad 4.949 \cdot \exp\{-21.543E(\mathbf{x})^{-0.804} \cdot (z - z_{th}(E(\mathbf{x})))\} \quad , z_{th}(E(\mathbf{x})) \le z \end{cases}$$

$$\begin{aligned} A'(E(\mathbf{x})) &= -206.09(E(\mathbf{x})/1000)^3 + 52.017(E(\mathbf{x})/1000)^2 + 19.301(E(\mathbf{x})/1000)[\mu\text{m/min}] \\ z_{th}(E(\mathbf{x})) &= 14.9(E(\mathbf{x})/1000) - 4.023[\mu\text{m}] \end{aligned} \tag{4}$$

4.2 Single exposure optimization method

In this paper, a pyramid microstructure as shown in Fig. 6 was fabricated, and then they were evaluated. Optimization was conducted under the condition of error requirement of less than 1×10^{-4} μm^4 (Eq. (1)), and the mesh size of simulation domain is 1 μm × 1 μm × 1 μm. Figure 7a summarizes the combination of the three optimized process parameters, and Fig. 7b shows SEM images of the fabricated photoresist microstructure by the optimized process parameters. Figure 8a shows the RMS error and its dependence on focal position. Both the numerical and the experimental results revealed a similar trend and the minimum error was obtained at the same optimal focal position –8 μm. The local error distribution of simulated structure at the best focal position (Fig. 8b) exhibits good agreements with the target. From these results, the accuracy of 3D photolithography simulation tailored to the DMD-based grayscale lithography system was demonstrated, and the validity of proposed optimization method was confirmed.

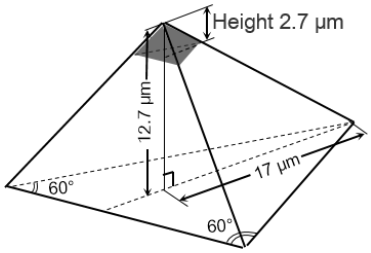

Figure 6. Pyramid microstructure used for the verification. The grayscale parts represent the critical features where the fabrication accuracy needs to be further improved by a variable weight factor.

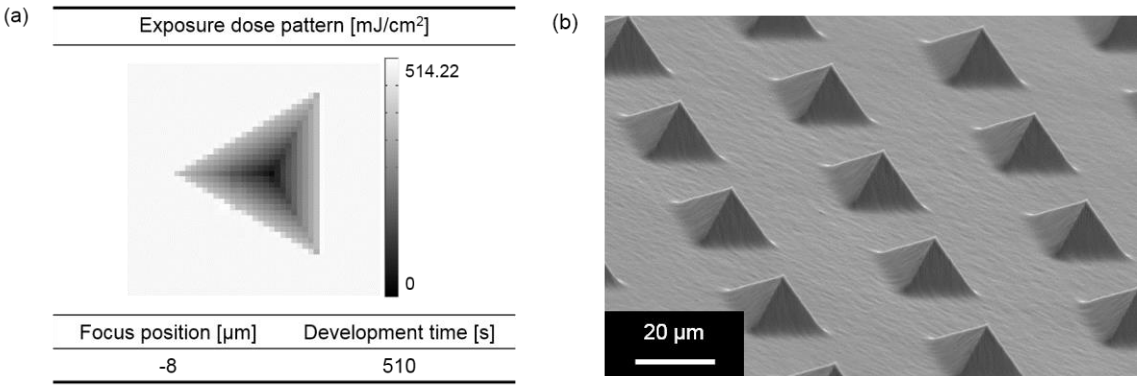

Figure 7. (a) Optimized parameters for pyramid structure. (b) SEM images of the fabricated photoresist microstructures.

Figure 8b shows the unsigned error distribution map between target and fabricated microstructure. The result shows good agreement after optimization. However, the top part of pyramid still shows errors. In practical applications, a

critical feature of the 3D microstructure may be more important and required to improve a fabrication accuracy. Until now, optimization was conducted with a uniform weight factor, i.e. setting $w(\mathbf{x}) = 1$ in Eq. (1) for the entire 3D microstructure. For critical feature, increasing the weight factor will tighten the accuracy requirements, locally. Figure 9a shows the location of challenging features where the fabrication accuracy needs to be improved, by subsequent increase of the weight factor. Figure 9b shows the results of the simulation and the experiment for different weight factor settings for the pyramid. As the weight factor increased from 1 to 10, the RMS error of the critical feature in both simulated and fabricated microstructures were decreased by increasing the weight factor, and the experimental RMS error was reduced by 63.3%. These results demonstrated that by adopting a variable weight factor in Eq. (1), precision of a critical feature on 3D microstructure can be effectively improved.

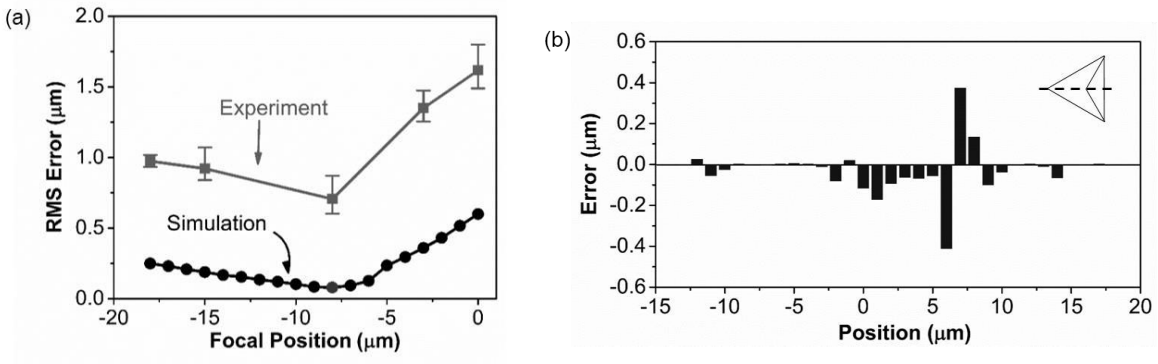

Figure 8. (a) RMS error for different focal positions of simulation and experimental results of the pyramid. (b) Local error distribution between the simulated microstructure and the target at the cross section.

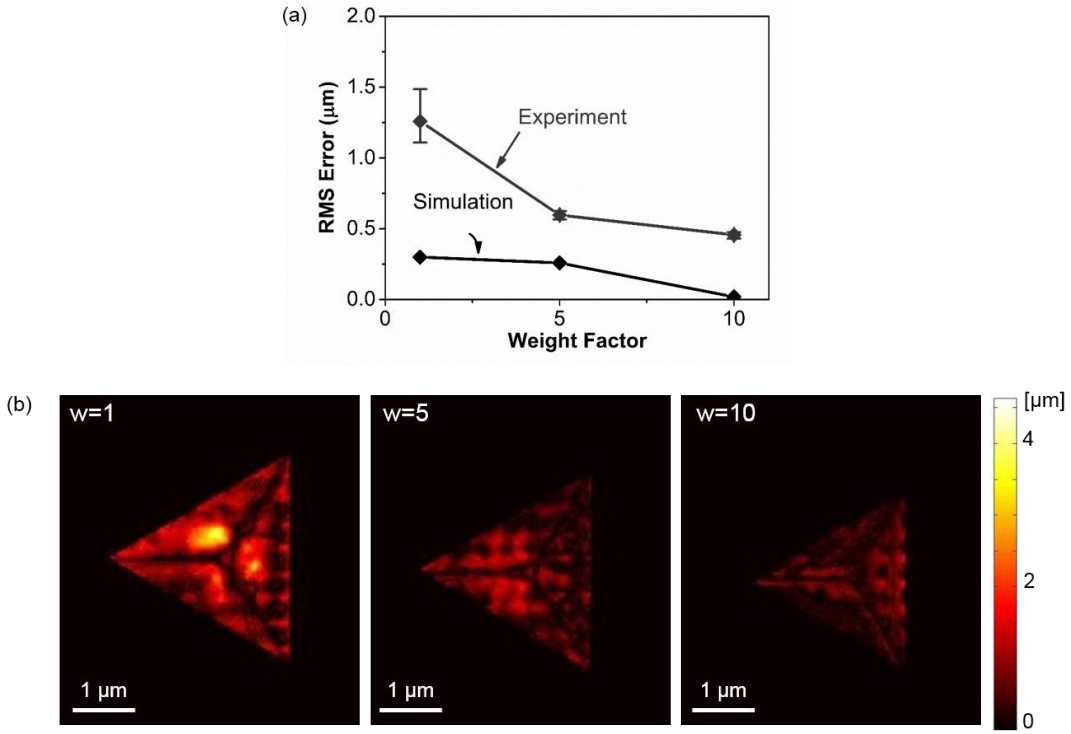

Figure 9. Simulation and experiment results for the pyramid with different weight factors. For weight factor increased from 1 to 10, charts here stand for (a) RMS error of critical feature in both simulated and fabricated microstructures. Experimental values represent averages and the minimum and maximum from five samples. (b) Unsigned error distribution of fabricated microstructures.

4.3 Multiple exposure optimization method

The multiple exposure optimization method is based on a qualitative analysis; better optimization result can always be obtained around focal position comparing to area out of the DOF. Further evaluation of single exposure optimization leads to this conclusion. Figure 10 shows cross sectional profiles of simulated structures for different focal positions. The simulated profiles around focal position got higher accordance with the target. An increasing mismatching was observed at the bottom part of pyramid when focal part shifts far away from the bottom, while an increasing accuracy was also confirmed for the top portion at the same time.

Figure 11a shows the comparison of optimization results between two methods. Higher accordance with target microstructure and accuracy uniformity were successfully confirmed. The RMS error decreased from 0.07919 μm to 0.0407 μm. This results indicated that the multiple exposure optimization method is a promising strategy to further improve precision for thicker photoresist structure. Figure 11b indicates the relationship between the RMS error and segment interval. When segment interval is smaller than the optics' DOF (3.3 μm) of the employed DMD-based grayscale lithography system, higher accuracy was realized by the multiple exposure optimization method. However, when the segment interval became larger than DOF, the RMS error of the multiple exposure optimization method increased rapidly and exceeded that of the single exposure optimization method. These simulated results concludes that the validity of the multiple exposure optimization method has been confirmed and the segment interval should be set to a value smaller than the DOF for the purpose of fabrication accuracy improvement.

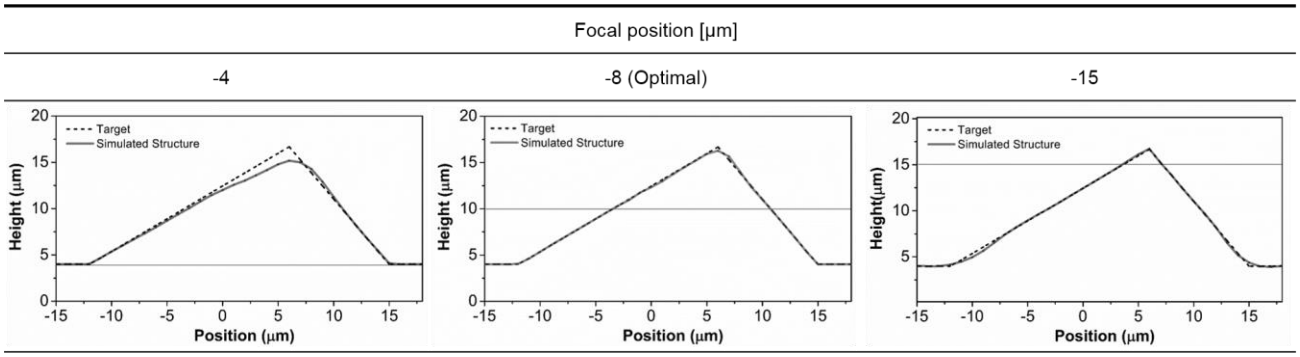

Figure 10. Cross sectional profiles for pyramid structure with optimized exposure dose patterns and development time at different focal positions. In the graph, focal position is indicated by gray solid line.

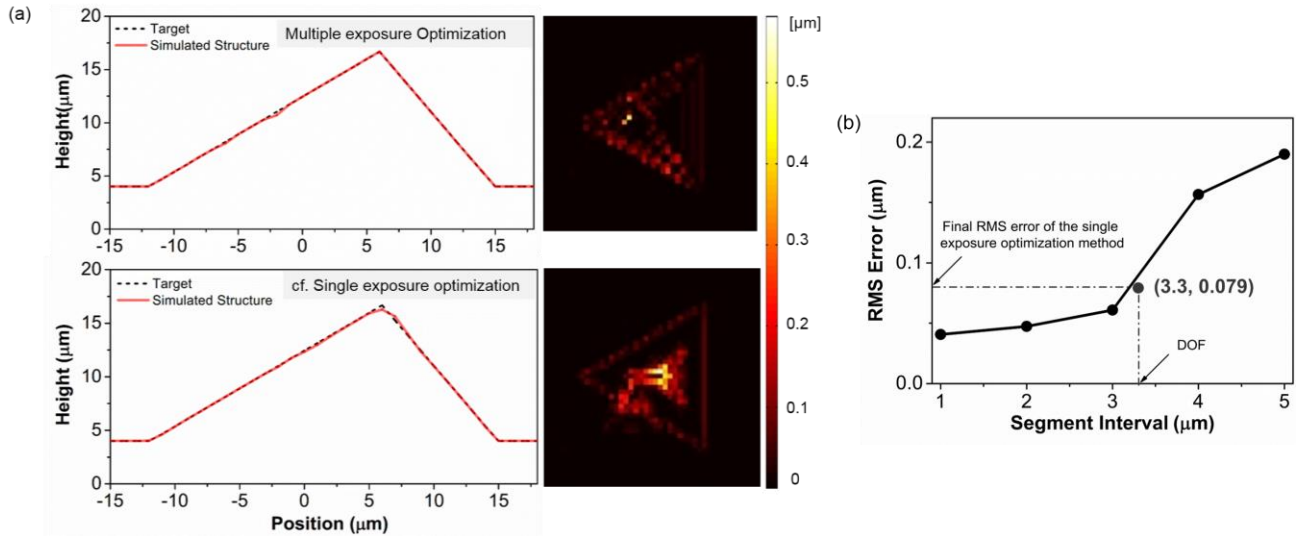

Figure 11. (a) Optimization result comparison between the multiple and single exposure optimization methods. (b) Relationship between the final simulation RMS error and segment interval.

5. CONCLUSIONS

In this paper, we presented a complete "input: target microstructure – output: process parameters" single and multiple exposure optimization methods for 3D microfabrication by means of a DMD-based grayscale lithography system. The developed optimization approach is based on 3D photolithography simulation and sensitivity analysis tailored to the DMD-based grayscale lithography system, and can optimize the combination of three important process parameters for positive photoresists: exposure dose pattern, focal position and development time. Meanwhile, a variable weight factor in the objective function was introduced to improve the fabrication accuracy of critical features. Through several experiments with the combination of the three optimized process parameters, the reliability of the 3D photolithography simulation, the validity and effectiveness of the single exposure optimization method, and the improvement of the fabrication accuracy were successfully confirmed. In addition, further simulation results demonstrated that the multiple exposure optimization method is the promising strategy to further improve precision for thicker photoresist structure. Consequently, the proposed two optimization methods have reached the state where they can successfully complement the difficult 3D microstructure fabrication using DMD-based grayscale lithography. Furthermore, the design time for many applications can be significantly reduced, while at the same time, fabrication accuracy and quality is improved. These presented optimization method will lead to new possibilities and prospects for 3D photolithography.

ACKNOWLEDGMENT

The authors wish to thank the staff at Tokyo Ohka Kogyo Co. Ltd. and NanoSystem solutions Inc. for the useful discussions, and Keyence Co. Ltd. for the support on the measurement. A part of this work was conducted at Kyoto University Nano Technology Hub for the "Nanotechnology Platform Project" sponsored by the Ministry of Education, Culture, Sports, Science and Technology (MEXT), Japan.

REFERENCES

[1] Waits, C. M., Modafe, A. and Ghodssi, R., "Investigation of gray-scale technology for large area 3D silicon MEMS structures," J. Micromech. Microeng.13, 170-177 (2003).
[2] Chung, J. and Hsu, W., "Fabrication of a polymer-based torsional vertical comb drive using a double-side partial exposure method," J. Micromech. Microeng. 18, 035014 (2008).
[3] Oppliger, Y., Sixt, P., Stauffer, J. M., Mayor, J. M., Regnault, P. and Voirin, G., "One-step 3D shaping using a gray-tone mask for optical and microelectronic applications," Microelectron. Eng. 23, 449-454 (1994).
[4] Hirai, Y., Inamoto, Y., Sugano, K., Tsuchiya, T. and Tabata, O., "Moving mask UV lithography for three-dimensional structuring," J. Micromech. Microeng. 17, 199-206 (2007).
[5] Totsu, K., Fujishiro, K., Tanaka, S. and Esashi, M., "Fabrication of three-dimensional microstructure using maskless gray-scale lithography," Sens. Actuators A, 130-131, 387-392 (2006).
[6] Zhong, K., Gao, Y., Li, F., Luo, N. and Zhang, W., "Fabrication of continuous relief micro-optic elements using real-time maskless lithography technique based on DMD," Opt. Laser Technol. 56, 367-371 (2014).
[7] Iwasaki, W., Takeshita, T., Peng, Y., Ogino, H., Shibata, H., Kudo, Y., Maeda, R. and Sawada, R., "Maskless lithographic fine patterning on deeply etched or slanted surfaces, and grayscale lithography, using newly developed digital mirror device lithography equipment," Jpn. J. Appl. Phys. 51, 06FB05 (2012).
[8] Morgan, B., Waits, C.M., Krizmanic, J. and Ghodssi, R., "Development of a deep silicon phase fresnel lens using gray-scale lithography and deep reactive ion etching," J. Microelectromech. Syst. 13, 113-120 (2004).
[9] Mack, C. A., "Fundamental principles of optical lithography," New York: Wiley, (2007).
[10] Mack, C. A., "Thirty years of lithography simulation," Proc. SPIE 5754, 1-12 (2005).
[11] Kempen, F., Hirai, Y., Keulen, F. and Tabata, O., "Automatic process design for 3D thick-film grayscale photolithography," Proc. Transducers2013, 1625-1628 (2013).
[12] Arfken, G. B. and Weber, H. J., "Mathematical Methods for Physicists," Amsterdam: Elsevier Academic Press, 489-497 (2005).
[13] Liu, C., Guo, X., Luo, B., Duan, X., Du, J. and Qiu, C., "Imaging simulation of maskless lithography using a DMD," Proc. SPIE 5645, 307-314 (2005).

[14] Ding, X., Ren, Y., Gong, L., Fang, Z. and Lu, R., "Microscopic lithography with pixelate diffraction of a digital micro-mirror device for micro-lens fabrication," Appl. Opt. 53, 5307-5311 (2014).
[15] Born, M. and Wolf, E., "Principles of optics: electromagnetic theory of propagation, interference and diffraction of light," Cambridge: Cambridge University Press (1999).
[16] Sethian, J. A., "Level set methods and fast marching methods," Cambridge: Cambridge University Press (1999).
[17] Keulen F., Hirai, Y. and Tabata, O., "Automated optimization of light dose distribution for moving-mask lithography," Proc. EuroSimE 2009, 1-9 (2009).
[18] Sensu, Y., Isono, M., Sekiguchi, A., Kadoi, M. and Matsuzawa, T., "Study of proximity lithography simulations using measurements of dissolution rate and calculation of the light intensity distributions in the photoresist," Proc. SPIE 5376, 1040-1052 (2004).
[19] Hirai, Y., Sugano, K., Tsuchiya, T. and Tabata, O., "A three-dimensional microstructuring technique exploiting the positive photoresist property," J. Micromech. Microeng. 20, 065005 (2010).